Calibration of Vessel Mounted LiDAR

Alan PICARD, Thomas TOUZÉ, Nicolas SEUBE, France
Jean-Guy NISTAD, Mathieu RONDEAU, Canada

SUMMARY

The use of Vessel Mounted Lidar (VML) and Multibeam echosounders has been motivated by an infrastructure inspection problem. The main challenge in this type of applications is to produce coherent data sets with centimetre accuracy, which cannot be achieved by using a traditional calibration procedure. The aim of this paper is to propose a methodology for accurate VML boresight angle calibration. As time synchronization may affect the data accuracy, we first describe a latency calibration estimation method, able to determine the total latency between any ranging sensor (VML or MBES), the IMU and the acquisition system. Then, we propose a new boresight angle calibration method between the LiDAR and the IMU, and we estimate its accuracy and precision. As these two methods do not need any positioning data, they avoid the propagation of GPS errors into the calibration procedure.

Key words: LiDAR, Boresight calibration, Latency calibration, Patch test, Marine Infrastructure surveys.

1. INTRODUCTION AND BACKGROUND

In the framework of marine infrastructure surveying, kinematic LiDAR (Light Detection And Ranging) are commonly used in order to accurately model topographic information. These ranging systems return detection points in the sensor frame which are geo-localized thanks to orientation angles given by an inertial motion unit (IMU) and GPS information. Most of the literature aiming at improving data quality from airborne, ground based or vessel mounted LiDAR focus generally on boresight angles calibration, self-calibration or radiometric correction. Self-calibrating a system (for instance a LIDAR-IMU system) consists in determining LIDAR range and angle biases simultaneously with LIDAR-IMU mounting angles [Gruen and Beyer, 2001]. In the field of boresight calibration, we can distinguish two classes of methods : tie points method, which uses known points observed with different attitudes to determine the boresight angles which maximizes the spatial coherence of the original data set [Morin and Naser El-Sheimy, 2002; Glennie, 2007; Filin, 2003]. Other methods use surface matching (i.e. digital elevation model matching) in order to detect and compensate for misalignment angles [Skaloud and Litchi, 2006; Schenk, 2001; Kumari et al., 2011]. Note that the classical patch-test procedure used in the hydrographic surveying framework falls into this latter class of methods.

In most of these works, latency between the orientation data from the IMU and detection points from the ranging system is not taken into account. In (Skaloud and Litchi, 2006), bore-sight angle determination is performed without any a priori latency calibration. As a matter of fact, poorly assessed latency may not impact data in optimal survey conditions e.g. few variation of the platform attitude. In that case, systematic errors due to bore-sight are not mixed with timing errors and their determination remains reliable. However, this latency plays a crucial role in the georeferenced data quality in high dynamics platform conditions. In (Skaloud, 2006), synchronization issues, as well as bore-sight angle lever-arms determination are identified as sources of errors. For meeting high-quality standards in the airborne LIDAR framework, (Skaloud, 2006) gives a maximum latency accuracy of 0.1ms between orientation and ranging data. As mentioned in (Filin and Vosselman, 2004), elimination of the systematic errors from survey data can be done by two different approaches: The first lies in analyzing each component of a survey system (ranging system, inertial motion unit, positioning system, acquisition software), and characterizing individual errors from all sensors.
Another approach is to identify systematic errors from geolocalized data, which happens to be corrupted by a coupled and non linear combination of sensors errors. These methods aim at retrieving systematic errors by inversion methods. However, errors may be highly dependent on the orientation dynamics of the platform. If it is actually the case, non corrected time synchronization errors may contribute significantly to the non observability of systematic errors.

Despite the fact that timing error is a major problem for calibrating properly a survey system, a quite small amount of work has been devoted to its determination. In [Hughes Clarke, 2003] the author analyses the possible source of undulations of outer beam data for multibeam echosounders, including time delays between motion sensors and multibeam systems. This effect can be enhanced by the fact that for deep water surveys, the time of flight of the acoustic return may be very different from outer beams and from nadir beams. This implies that time stamping of the attitude value for a complete swath is not a unique time stamp but would depend on the time of arrival of the acoustic return. An analysis of wavelet presence, correlated with roll value of the motion is presented in order to help the hydrographer to identify a possible time delay problem in its datasets. Some other approaches, implemented in hydrographic acquisition software propose to the user to correlate the outer beams of the ranging device to the roll and/or pitch time series. By determining a phase error between the two signals, one can estimate the timing error between the motion sensor and the ranging sensor. The main drawback of this approach lies in the fact that the survey must be conducted over a at terrain, in order to eliminate the possible effect of terrain undulations that could be interpreted as timing errors. The other drawback is the accuracy of the latency estimation is relatively poor.

2. LIDAR-IMU LATENCY CALIBRATION PROCEDURE

In this section, we propose a method that can be used for estimating the IMU latency with respect to a ranging system, connected to acquisition software. Latency between a ranging system and an IMU can be determined by applying a controlled rotational motion to the ranging system and by estimating the position shift of a spherical target induced by a rotational motion. Hereafter, we shall describe a possible set-up in the case of a LiDAR coupled to a motion sensor. For doing so, it is required to get the following data:

- Position of the ranging system optical center through time;
- Orientation of the IMU frame with respect to the navigation frame. It is to be mentioned that the orientation bias between the IMU frame and the LIDAR is not required at this stage, and will be investigated later;
- Scan lines (e.g. set of detection points) from the LIDAR;
- Angular velocities of the LIDAR-IMU system.

Angular velocities provided from the IMU are submitted to the same latency that we would like to estimate. Therefore, it is preferable to use an external source of angular velocity. We chose to use a 3D motion simulator capable of measuring angles with high accuracy, and to control very precisely angular velocities. In the following, we suppose that angular velocities are available with very high accuracy.

Let us denote by $n = (N,E,D)$ the navigation frame with origin at the motion simulator center of rotation, by *bS* the kinematic LiDAR body frame, and by *bI* the inertial motion unit frame. Let us first observe that latency estimation is not affected by orientation bias from the IMU frame and the kinematic LiDAR frame. Let us denote by M a LiDAR detection point, referenced from its optical center *O* in its own frame *S*, and $x_f = OM_f$ in a frame *f*. In the navigation frame, we can write for a static (or quasi static) kinematic LiDAR detection point

$$x_n = R_{bI}^{n} R_{bS}^{bI} x_S \qquad (1)$$

where R_{bI}^{n} and R_{bS}^{bI} are direction cosine matrix from frame (*bI*) to (*n*) and (*bS*) to (*bI*).

Now consider the same scene, but seen from the kinematic LiDAR in rotational motion. The principle of the method is to consider that point *M* has been detected by the LiDAR, but shifted in the navigation frame. Let *M'* be the image of point *M*, the kinematic LiDAR being in rotational motion. Denoting by $x'_f = OM'_f$, we can write

$$x'_n = R_{bI}^{n}(t-dt) R_{bS}^{bI} x_S \qquad (2)$$

From (1) and (2), we deduce that

$$x_n = R_{bS}^{bI} R_{bI}^{n}(t-dt) x'_n$$

Assuming that the rotational motion is with a constant angular velocity, and after some manipulations, we obtain the relationship between latency and the displacement vector $\Delta_n = x_n - x'_n$ due to the rotational motion:

$$dt = \frac{\|\Delta_n\|}{\|\omega_{bI/n}^{bI} \wedge x'_n\|}$$

where $\omega_{bI/n}^{bI}$ denotes the angular velocity of the LiDAR-IMU with respect to the (n) frame, expressed in the IMU coordinate system.

3. EXPERIMENTAL RESULTS OF THE LATENCY CALIBRATION METHOD

The problem is now to define a reference point M that can be defined from a LiDAR scan. A good candidate for such a point is the center of a spherical target. Indeed, this center can easily be fitted by LiDAR returns from the sphere surface with a very high accuracy. By an iterative least-squares procedure, one can accurately estimate a sphere center from surface points [Grejner-Brzezinska, 2011]. In figure 1, we plotted LiDAR return from a spherical target used in our experimental set-up.

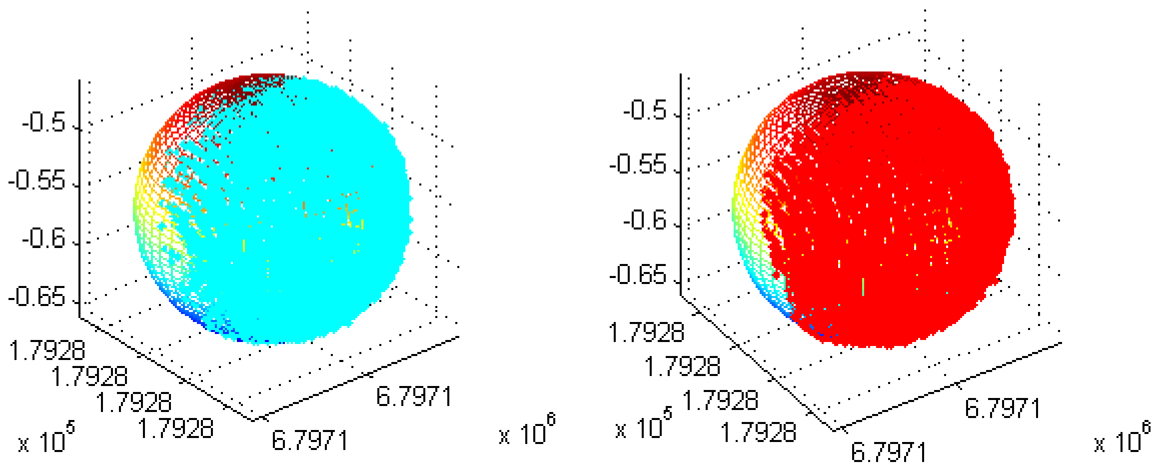

Figure 1: Spherical targets scans. Right side 7 deg/sec scans, left side -7deg/sec scans. Position shift of the centers has been estimated with a precision of 0,04 mm.

Our method aims at being a laboratory test and will not require any positioning device, which will therefore not propagate positioning errors in the calibration itself. The experimental set-up that we realized is formed by a Leica HDS6200 Laser scanner, coupled with an OCTANS 4 Attitude sensor (they are mounted in the same mechanical bracket – figure 2). The IMU and the LiDAR have been installed on an IX-Motion TRI30 motion simulator, able to achieve rotational motions with a high precision and accuracy (about 0.001 deg/sec).

A spherical target of diameter 20cm has been placed at 2,5 metre from the LiDAR, and the LiDAR-IMU system was tasked to make a series of 30 alternate scans of the sphere at a velocity of ± 7 deg/sec. Sphere center shift Δ_n for each velocity (+7, -7) has been used in order to estimate the latency dt.

Figure 2: Experimental set-up for latency calibration: The Leica HDS6200 and the IxSea Octan4 are mounted on a IXMotion TRI30 motion simulator, scanning a sphere of precision.

Both LiDAR and IMU data were gathered by the Qinsy acquisition software. It should be mentioned that our method estimates the total latency between the IMU, the LiDAR and the acquisition PC. In order to check for the latency induced by the PC acquisition buffer size, we made several tests with different software configurations. Indeed, as the OCTANS4 was not connected to a Pulse per Second signal, and data were transmitted through a serial link, the size of the serial link buffer might impact the total latency. Data from these tests are given in table (1).

The latency of the OCTANS 4, when connected by a serial link, is around 2,35 ms with 0,2ms uncertainty with 1σ confidence interval. The latency due to buffering should be added (see [QPS, 2007] for a review of the effect of buffering on latency), and the latency due to data assimilation by Qinsy in order to get the total latency. Table (1) gives the results we obtained with several buffer configurations, in order to check the impact of various buffer size and our latency estimate resolution.

One can check that the residual latency (i.e. the latency due to the acquisition software) and data assimilation is quite constant, with an accuracy of 0,2ms. Note that figures given in table (1) are averaged values of a series of runs, which returned the latency estimate with SD values of about 0,1ms. We can conclude from these tests that the method is able to find IMU latency with an accuracy of 0,2ms and a precision of 0,01ms.

It is also very important to mention that this method applies to any IMU connected to an acquisition system, and does not depend of the ranging device (LiDAR or MBES). Therefore, hydrographic survey systems and IMU's latency can be estimated by using this method, which is a positioning-error-free calibration method.

Table 1: Latency estimation results

FIFO buffer size	Sphere center SD	Total latency	OCTANS 4 latency	Buffer latency	Residual latency
0	0,041mm	2,82ms	2,35ms	0	0,47ms
8 bytes	0,044mm	3,31ms	2,35ms	0,69ms	0,27ms
14 bytes	0,042mm	3,97ms	2,35ms	1,22ms	0,40ms

4. LIDAR-IMU BORESIGHT ANGLES CALIBRATION PROCEDURE

The approach we present here is devoted to LiDAR-IMU boresight calibration procedure independent of any positioning data; namely, we do not want positioning errors to corrupt the calibration procedure.

4.1 Principle of the method

The procedure we propose for LiDAR-IMU boresight angle calibration is motivated by the fact that we would like to eliminate the influence of positioning errors on the misalignment angle computation. The procedure we propose can be achieved in a laboratory, and requires to make a series of static scans of a tripod (see figure 3) target from several points of views.

Let us suppose that the LiDAR and the IMU are rigidly mounted in a mechanical bracket. We start by a first static scan of the tripod. The major advantage of this type of target lies in the fact that its orientation can be determined only from the knowledge of the intersection points (C_1, C_2, C_3) between the LiDAR scanning plan and the tripod itself. Points (C_1, C_2, C_3) can be determined by fitting the center of the ellipse produced by the intersection of the LiDAR scanning plan and the tripod cylinders. By using notations defined in figure (1), it can be readily shown that for all $i, j \leq 3; i \neq j$ we have

$$d_{ij}^2 = d_{0\mathrm{i}}^2 + d_{0\mathrm{j}}^2 - 2\mathrm{d}_{0\mathrm{i}} d_{0\mathrm{j}} \cos\theta_{ij}$$

These three non linear equations can be numerically solved for $(d_{0\mathrm{i}})_{i=1...3}$, with prior knowledge of the three angles forming the tripod. Then, we can estimate the tripod center O, being the intersection of three spheres of centers (C_1, C_2, C_3) with radius (d_{01}, d_{02}, d_{03}).

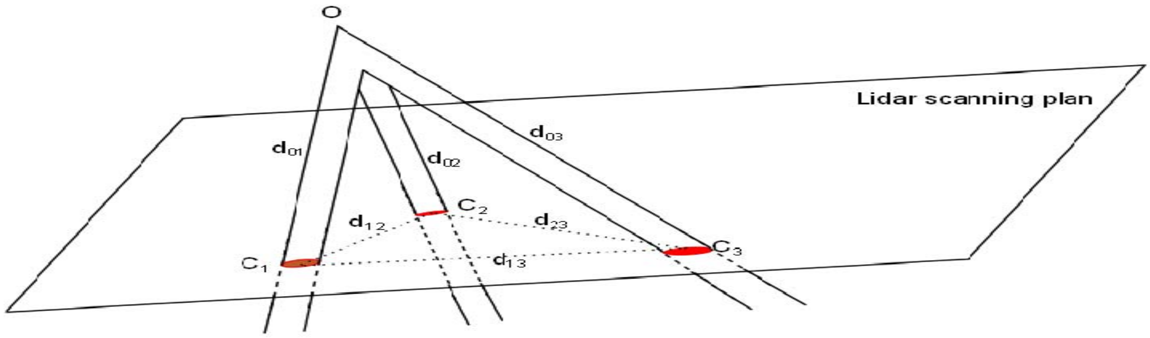

Figure 3: Geometric view of the bore-sight calibration target

Let us denote by (x_0, y_0, z_0) the coordinates of point O in a frame attached to the Lidar scanning plan, and $(x_i, 0, z_i)$ the coordinates of points C_i. Then, we have

$$(x_0 - x_i)^2 + y_0^2 + (z_0 - z_i)^2 = d_{0i}^2, i = 1..3$$

this last system being explicitly solved for (x_0, y_0, z_0) by

$$(x_0 - x_1)^2 + y_0^2 + (z_0 - z_1)^2 = d_{01}^2$$
$$2x_0(x_2 - x_1) + 2z_0(z_2 - z_1) = d_{01}^2 - d_{02}^2 + x_2^2 - x_1^2 + z_2^2 - z_1^2$$
$$2x_0(x_3 - x_1) + 2z_0(z_3 - z_1) = d_{01}^2 - d_{03}^2 + x_3^2 - x_1^2 + z_3^2 - z_1^2$$

We observe that y_0 has two solutions, which express the fact that the tripod center may be located in the two half space separated by the Lidar scanning plane. Knowing the coordinates of point O, we can reconstruct the directions OC_i of each tripod foot in the Lidar scanning plane.

Let us now suppose that two different static scans of the tripod have been performed, for two different Lidar orientations. For a given orientation i let us denote by $X_{bSi} = OC_i$ the tripod foot vectors coordinated in the LiDAR frame *bS*. Note that each of these vectors can be uniquely attached to a given footprint whenever the diameters of the foot tube are different.

4.2 Derivation of the bore-sight calibration equations

Consider now two different foot vectors X_{bS_1}, X_{bS_2} obtained from two orientations of the LiDAR scanning plan towards the tripod. Let us denote by

$$R_{bS}^{bI}(\varphi,\theta,\psi)=\begin{pmatrix} cos\,\psi\cos\theta & cos\,\psi\sin\theta\sin\varphi+\sin\psi\cos\varphi & -cos\,\psi\sin\theta\cos\varphi+\sin\psi\sin\varphi \\ -sin\,\psi\cos\theta & -sin\,\psi\sin\theta\sin\varphi+\cos\psi\cos\varphi & \sin\psi\sin\theta\cos\varphi+\cos\psi\sin\varphi \\ \sin\theta & -\cos\theta\sin\varphi & \cos\theta\cos\varphi \end{pmatrix}$$

the direction cosine matrix defining the rotation from the LiDAR frame bS to the IMU frame , namely, the boresight angle direction cosine matrix parameterized by Euler angles (φ,θ,ψ);
$(\varphi_0,\theta_0,\psi_0)$ an a priori estimate of the boresight angles;
$R_{bI\,i}^{n}$, the direction cosine matrix from the IMU frame to the navigation frame n (i.e. the local geodetic frame (North, East, Down)) from the observation site i.

The basic principle of our method is to express that in the navigation frame n, the tripod foot vectors $R_{bI}^{n_i}X_{bI_i}=R_{bI}^{n_i}R_{bS}^{BI}X_{bS_i}$, coordinatized in the navigation frame are invariant for each LiDAR static scan. Therefore, the fundamental equation for this calibration method is

$$R_{bI}^{n_1}X_{bI_1}=R_{bI}^{n_2}X_{bI_2}\ ,$$

We start with
$X_{bI_i}=R_{bS}^{bI}X_{bS_i}:=g(\varphi_0,\theta_0,\psi_0)$. In considering a linear approximation of this equation, we obtain: $g(\varphi,\theta,\psi)=g(\varphi_0,\theta_0,\psi_0)+g'(\varphi_0,\theta_0,\psi_0)\cdot(\varphi-\varphi_0,\theta-\theta_0,\psi-\psi_0)^T$, which leads to the following linear system

$$R_{bI}^{n_1}g(\varphi_0,\theta_0,\psi_0)_1-R_{bI}^{n_2}g(\varphi_0,\theta_0,\psi_0)_2=(R_{bI}^{n_1}g'(\varphi_0,\theta_0,\psi_0)_1-R_{bI}^{n_2}g'(\varphi_0,\theta_0,\psi_0)_2)(\Delta\varphi,\Delta\theta,\Delta\psi)^T$$

In combining three observation sites, we obtain nine equations, which can be solved by weighted least squares[1] which returns approximate values of (φ,θ,ψ). Then, by updating $(\varphi_0,\theta_0,\psi_0)\leftarrow(\varphi,\theta,\psi)$, we create a sequence of estimated boresight angles. Convergence of this process is not guaranteed but generally occurs after a few iterations.

[1] The weight matrix depending on the confidence in the estimation of the coordinates of the foot vector (which comes from the ellipse center estimate) and from the precision of the IMU which delivers the direction cosine matrix.

5. ANALYSIS OF THE BORESIGHT CALIBRATION METHOD

5.1 Description of the simulation set-up

In order to study the robustness and performance of the boresight calibration method, a simulation of the whole estimation process has been performed for checking the boresight angle values with respect to some uncertainty on the ellipse center estimates. In this set-up, we considered a tripod with a 60 deg angle with respect to its vertical axis, and we generated a sequence of 3 LiDAR scanning plans given by the following rotations in roll, pitch and heading:

$$(\varphi,\theta,\psi) = [-20{,}0{,}30],[0{,}20{,}120],[20{,}-20{,}240]$$

The uncertainty on the ellipse center was estimated by a statistical analysis of the least-squares residuals and was set to 1mm and 1cm for a tripod tube of diameter 10cm.

5.2 Performance and Robustness analysis

From figures 4 and 5, it can be seen that our estimation method is unbiased. One should mention that the method presented in [Grejner-Brzezinska, 2011] induced a bias in the boresight matrix estimation since this method is based on a composition of micro-rotators which is no more a true direction cosine matrix representing a rotation matrix.

The following results show frequency distribution graphs of the roll, pitch and yaw errors for several ellipse centre distribution errors. It can be seen (figure 5) that for a realistic error distribution on the ellipse centers (about 1mm), the boresight angle errors are less than 0,01 deg on pitch and roll, and 0,05 deg for the heading angle. Our simulation results indicate that this method converges in a few iterations, generally less than five. The robustness of the method can be checked in figure 4: even in the case of 1cm (this error is clearly over estimated) of ellipse center error, boresight angles are quite well estimated, with an error of less than 0,1 deg for pitch and roll and less than 0,5 deg for heading.

From these simulation results, we observe that the estimation procedure including ellipse detection uncertainty, geometric reconstruction of the tripod foot vectors, and boresight matrix estimation is unbiased and very accurate, in comparison of classical surface matching methods, which accumulate latency errors due to kinematic survey, positioning errors, and surface modeling errors.

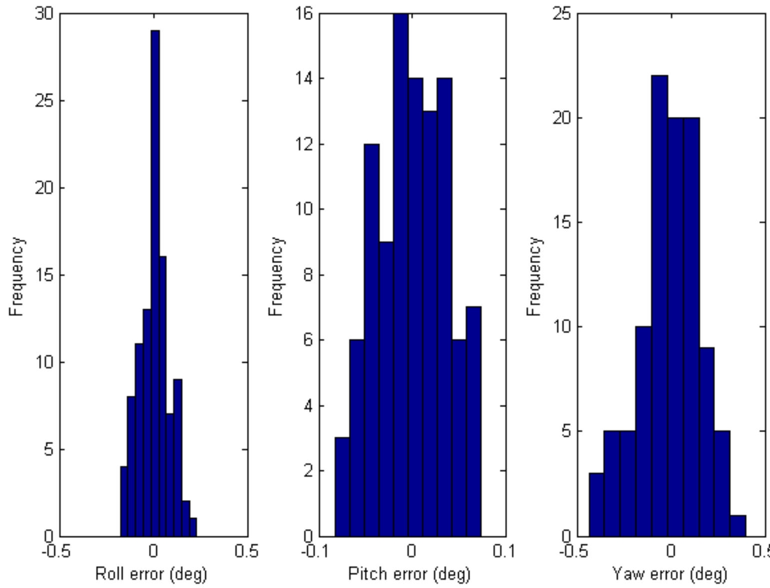

Figure 4: Boresight errors with 1cm uncertainty on ellipse centers

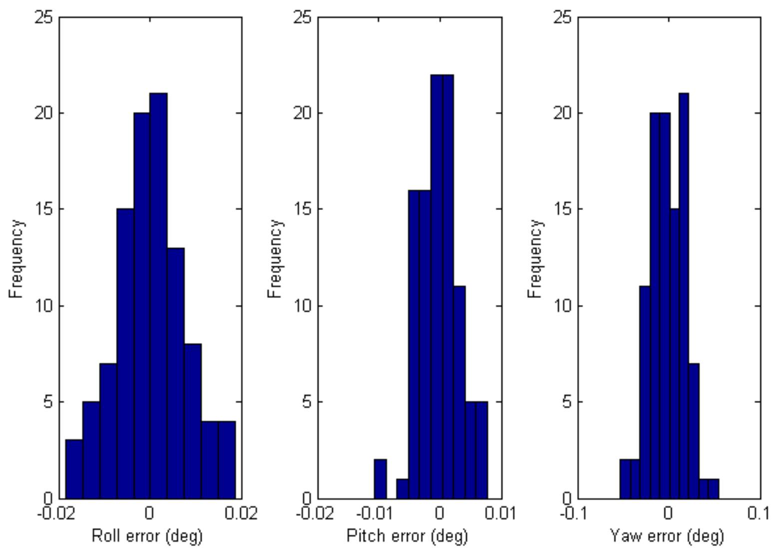

Figure 5: Boresight errors with 1mm uncertainty on ellipse centers

6. CONCLUSION

The LiDAR calibration methods we propose offers many advantages in comparison to field calibration methods: they save survey mobilization time and they are free of any positioning errors, which is not the case of surface matching methods and target methods. They also avoid the classical obstruction and loss of accuracy due to calibration on edged targets. The boresight calibration method we propose is also free of inertial measurement errors due to eventual fast dynamics motion, as it only requires a series of static scans.

The latency calibration approach may be applied to any IMU and acquisition software, independent of the ranging sensor (LiDAR or MBES). The boresight calibration procedure is for the moment limited to LiDAR, but could be also adapted to MBES calibration.

REFERENCES

[Filin, S., 2003] Recovery of systematic biases in laser altimetry data using natural surfaces. Photogrammetric Engineering & Remote Sensing 69, 1235-1242.

[Filin, S., Vosselman, G., 2004] Adjustment of airborne laser altimetry strips. In: ISPRS Congress Istanbul, Proceedings of Commission III.

[Glennie, C., 2007] Rigorous 3d error analysis of kinematic scanning lidar systems. Journal of Applied Geodesy 1, 147-157.

[Grejner-Brzezinska, D. A., Toth, C. K., Sun, H., Wang, X., Rizos, C., Nov 2011] A robust solution to high-accuracy geolocation: Quadruple integration of GPS, IMU, pseudolite, and terrestrial laser scanner. IEEE Transactions on instrumentation and measurement 11, 3694-3708.

[Gruen, A., Beyer, H., 2001] Calibration and Orientations in Computer Vision. Springer, Ch. System Calibration through Self-Calibration., pp. 163-193.

[Hughes Clarke, J., 2003] Dynamics motion residuals in swath sonar data: Ironing out the creases. International Hydrographic Review 4(1), 6-23.

[Morin, K., Naser El-Sheimy, N., 2002] Post-mission adjustment methods of airborne laser scanning data. In: FIG XXII Int. Congress, Washington DC.

[QPS, 2007] Timing in Qinsy. QPS BV, The Netherlands.

[Schenk, T., 2001] Modeling and analyzing systematic errors of airborne laser scanners. Tech. rep., Department of Civil and Environmental Engineering and Geodetic Science, The Ohio State University, Columbus, OH.

[Skaloud, J., 2006] Reliability of direct georeferencing: Phase 0. Tech. rep., Euro SDR commission 1: sensors, primary data, acquisition and georeferencing.

[Skaloud, J., Litchi, D., 2006] Rigorous approach to boresight self-calibration in airborne laser scanning. ISPRS Journal of Photogrammetry & remote Sensing 61,
47{59.

BIOGRAPHICAL NOTES

Nicolas SEUBE obtained a PhD in applied mathematics from Paris Dauphine University in 1992. His research interests are motivated by underwater technologies and hydrographic surveying. Since 2005, he is the coordinator of the ENSTA Bretagne hydrographic course (30 students at Master level), and developed a research group in bathymetry, hydrographic instrumentation and cartography. His present research interest includes cartography aware ship dynamics, hybrid positioning systems, inertial navigation, and uncertainty management in hydrographic surveying. Since 2011, he acts as scientific director of the CIDCO (Centre Interdisciplinaire de Développement de la Cartographie des Océans), Canada, Qc

Coordinator of the Hydrography/Oceanography Course
Professor at the ENSTA Bretagne, dept STIC/OSM
nicolas.seube@ensta-bretagne.fr

Alan Picard graduated from ENSTA Bretagne with a Master's degree in hydrographic surveying in 2011. Before graduating, he gained hydrographic experience with the dredging company Van Oord in Africa.

Since September 2011, he has been a research engineer in the Ocean Sensing and Mapping Lab of the ENSTA Bretagne. His research interests include advanced LiDAR calibration methods and hybrid navigation systems.

He will be enrolled in a PhD program in the framework of a collaboration research project with ENSTA Bretagne and IXSea concerning multisensor positioning in multi-path environments.

CONTACTS

Alan Picard, Thomas Touzé, Nicolas Seube
ENSTA Bretagne
2 rue François Verny
Brest

FRANCE
Tel. +33(0)2 98 34 88 88
Fax +33 (0)2 98 34 88 46
Email: nicolas.seube@ensta-bretagne.fr
Web site: http://www.ensta-bretagne.fr

Jean-Guy Nistad, Mathieu Rondeau
CIDCO
310, rue des Ursulines, C.P. 3300
Rimouski (Québec) G5L 3A1
CANADA
Tel. +1 418 725 1732 #1722
Fax +1 418 724 1401
Email: nistadj@cidco.ca
Web site: www.cidco.ca